Processes for Removal and Immobilization of ^{14}C, ^{129}I, and ^{85}Kr

Advanced Fuel Cycle Initiative

Prepared for
U.S. Department of Energy
Campaign or Program

DM Strachan SA Bryan
CH Henager TG Levitskaia
J Matyàš PK Thallapally
RD Scheele WJ Weber
Richard Zheng ***National Laboratories***

September 2009

PNNL-18852

Reviewed by:

Acting Director, Fuel Cycle Research and Development

Robert Price Date

Concurred by:

Director, AFCI Technical Integration Office

Phillip Finck Date

Approved by:

Deputy Assistant Secretary, Fuel Cycle Management

(AFCI Program Manager) Paul Lisowski Date

SUMMARY

There are methods that are current candidates for the removal and immobilization of ^{14}C, ^{129}I, and ^{85}Kr. These methods have been outlined by Gombert (Gombert II 2007) and are not covered in this white paper. The methods covered here are those suggested by the current state-of-the-art science that show promise for the removal or immobilization of these isotopes from an advanced fuel cycle reprocessing plant. For the purposes of this white paper, all processes suggested by Pacific Northwest National Laboratory scientists are considered. The number of these processes to be actively investigated is reduced through a preliminary grading so that a small research project can be carried out to obtain a data set with which further decisions about these technologies can be made. Some of the technologies considered here are only immobilization methods, while some are both removal and immobilization methods.

This white paper is organized in the following way. We first discuss each technology grouped under the specific isotope to be treated. Some technologies, of course, apply to more than one isotope. In the cases where the technology applies to more than one isotope, the technology is discussed under the isotope to which the technology is most applicable and reference is made in each of the other isotope sections to the section where the technology is thoroughly discussed. Each of the technologies is discussed in the framework of a literature search with proposed work. The objective of the literature search is to build the case for the applicability of the technology being discussed to the removal and immobilization of these isotopes. In the next section, we discuss our selection of the top four technologies. In the last section, we discuss the results from the initial studies on three of the four technologies. In sufficient progress was made with the nanotube concept to warrant reporting here.

CONTENTS

FIGURES

TABLES

WASTE FORMS PROCESSES FOR REMOVAL AND IMMOBILIZATION OF ^{14}C, ^{129}I, AND ^{85}KR

1. INTRODUCTION

While current technologies exist (Gombert II 2007) for the removal and immobilization of ^{14}C, ^{129}I, and ^{85}Kr from the off gas of nuclear facilities, there are other emerging methods based on current state-of-the-art science that show promise for the removal or immobilization of these isotopes from an advanced fuel cycle reprocessing plant. This white paper presents several processes suggested by Pacific Northwest National Laboratory. The number of these processes to be actively investigated is reduced through a preliminary grading. Small research projects were conducted on the down-selected processes to determine which technologies to pursue further. Some of the technologies considered here are only immobilization methods, while some are both removal and immobilization methods.

This white paper is organized in the following way. We first consider each isotope and discuss the technologies applicable to its treatment. Some technologies apply to more than one isotope, and in these cases, the technology is discussed under the isotope to which the technology is most applicable and reference is made to that discussion in the other isotope sections. Each of the technologies is discussed in the framework of a literature search establishing the technology's potential, identifying knowledge gaps, and proposing work to close them. In the Section 5, we discuss our selection of the top four technologies covering all gaseous radionuclides. In the last section, we discuss the results from the initial studies on three of the four technologies. Insufficient progress was made with the nanotube concept to warrant reporting it here.

2. Carbon-14

Three novel technologies relevant to ^{14}C removal are discussed here: silicon carbide formation, amino-sorbent biomaterials, and functionalized aerogels.

2.1 Immobilization with silicon carbide

Silicon carbide (SiC; see the Krypton-85 section for the more complete discussion) can also be used to immobilize ^{14}C. However, the ^{14}C needs to be trapped close to its main source. A reverse water shift reaction

$$CO + H_2 \xrightarrow{catalyst} CH_4 + H_2O \qquad (0.1)$$

can be carried out to convert the ^{14}CO or $^{14}CO_2$ to a hydrocarbon such as CH_4 or C_2H_6. In the formation of SiC by physical vapor deposition (PVD) or chemical vapor deposition (CVD), methyl-trichlorosilane, CH_3SiCl_3 (Jiangang et al. 2006) is reacted at elevated temperature to form bulk SiC. Incorporating ^{14}C into the methyl group for some of the CH_3SiCl_3 would allow the ^{14}C to be incorporated directly into the SiC matrix, thus forming $Si^{14}C$. While the formation of hydrocarbons from CO_2 is energy intensive, syngas, a mixture of CO and H_2 formed from the reaction of natural gas and steam, is routinely made and used to form higher molecular weight organic compounds. The benefits of this technique along with the formation of SiC would have to be balanced against the existing technique, i.e. precipitating as a carbonate followed by immobilization in cement. Silicon carbide has a much lower dissolution rate than cement and, hence, would have a lower release rate in a repository over the lifetime of the waste form.

2.2 Separation and Capture of ^{14}C with Amino-Sorbent Biomaterials

One possible method to separate and capture CO_2 is to use amino-sorbents. Absorption of CO_2 in aqueous amine solutions has been extensively used for the removal of CO_2 from gas streams in many industries. The downside to this method is that it requires energy-intensive wet chemical stripping of CO_2 and regeneration of the original material. Other drawbacks of aqueous amine scrubbing are solvent losses associated with the high volatility of amines, limited lifetime of the amine solution due to degradation through oxidation of the amine, and corrosion problems. Recently, several solid amine enriched sorbents have been synthesized and successfully tested to remove CO_2 from enclosed environments such as submarine, aircraft, spacecraft, and enclosed pressurized chambers. However, the high cost of these sorbents prohibits their large-scale application in the utility industry. Consequently, $^{14}CO_2$ separation and capture may benefit from the development of new economical amine-enriched sorbents.

Readily available amino-sorbents produced from biomass need to be investigated, with specific interest in chitosan and related materials for the capture of ^{14}C in CO_2 from off-gas streams. Chitosan materials have been previously shown to exhibit high affinity for CO_2. They are economical, safe, durable, easily regenerated, and useable on industrial scale. Chitosan has been widely used as a membrane material in pervaporation (evaporation through a membrane), dehydration, and gas permeation studies because of its high hydrophilic, good chemical, temperature, pressure, and mechanical properties. An important advantage of chitosan is that it can be engineered into different shapes and physical forms, such as nanoparticles, microspheres, membranes, sorption beads, etc. In addition, because of the amino- and hydroxy-functionalities, chitosan is relatively easily modified chemically, which can be implemented as needed to control its surface area, cross-linking, chemical, and mechanical properties.

Chitosan is produced by hydrolysis of chitin, a homopolymer composed of β-(1-4)-linked N-acetyl-D-glucosamine residues. It is one of the most abundant and renewable natural biopolymers, second only to cellulose. Chitin and chitosan have long been of commercial interest because of their high nitrogen content (~7 mass%) compared to synthetically substituted cellulose (~1 mass%). Chitin is an inexpensive, non-toxic natural polymer that is easily deacylated to generate chitosan.
Chitin and chitosan are primarily manufactured from the shells of crab and shrimp, which are a waste product of the food industry and, therefore, relatively inexpensive. Alternately, in the case of large scale demand, fungal sources, such as mycelia, could be cultivated as a source of chitin and chitosan. Fungal sources can be continuously cultivated, rapidly fermented, and produced with consistent composition that would not require demineralization as do shells.

3. Iodine-129

Two technologies are relevant to the removal and immobilization of ^{129}I – Functionalized Aerogels and Silver-Loaded Zeolite (see Section 4.2)

3.1 Functionalized Aerogels for Capture and Immobilization of ^{129}I, ^{85}Kr, and $^{14}CO_2$

Aerogel materials, both silica- and carbon-based, have a promising potential for use in the capture of gaseous radionuclides ^{129}I, ^{85}Kr, and ^{14}C (see Section 2.1) from off-gas stream because of their high surface area, high porosity, ease of functionalization with organosilane chemistry (Fryxell et al. 2007), adequate mechanical and chemical durability, and temperature stability. The highly porous nature of an aerogel structure provides a high surface area - in excess of 500 m^2/g, with 3000 m^2/g with thermal activation. The micropores provide excellent conditions to physically adsorb the waste components by van der Waals or London dispersion forces, which can be leveraged to provide additional time for reaction with the chemically functional constituent. Because sol-gel processing (Figure 1) is used to

make aerogels, their chemical makeup can be easily tailored for specific radionuclides. The ability to modify the surfaces of an aerogel with chemicals (monolayer coating) that have one end bonded to the aerogel substrate and the other end with the desired chemical or "functional" group providing the high-affinity and selective chemisorption sites for specific gaseous radionuclides from off-gas. Chemical modification with organosilanes can take place during the sol-gel processing (Burkett, Sims, and Mann 1996; Fowler, Lebeau, and Mann 1998; Lebeau et al. 2000), thus providing a novel pathway to perform the modification during the solvent displacement stage. A strategy patented by PNNL researchers to decorate the free-standing aerogel structure after drying can also be used (Zemanian, Fryxell, and Ustyugov 2006).

The advantage of this functionalization strategy is that it can be tailored for multiple targets simply by varying the chemical nature of the organosilane. At PNNL there is significant experience with chemically modifying nanoporous architectures with organosilanes that self-assemble in supercritical fluid (SCF) media (Zemanian et al. 2001). These chemical modifications of aerogels strengthen the aerogel structure and passivate the interface towards corrosion/degradation, significantly improving their overall chemical and mechanical stability.

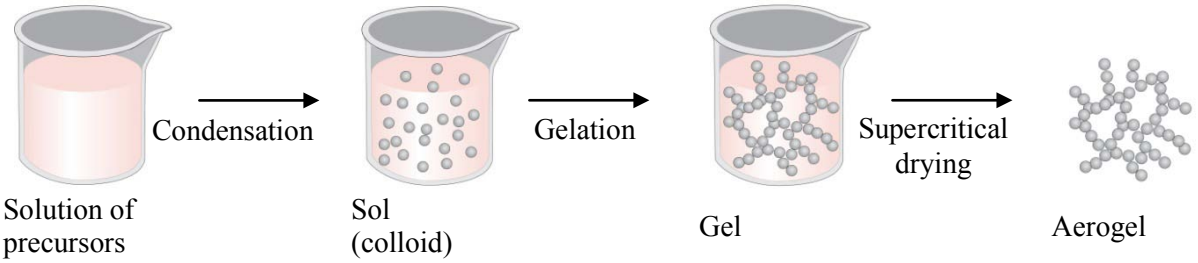

Figure 1. Schematic Outline for Preparation of Aerogel by Sol-gel Process

In addition to high adsorption capacity for gases, the physical structure (i.e. porosity) of silica aerogels can be altered with sintering, isostatic compression, or a combination of both. The microporous network of silica aerogels can be quickly sintered at low temperatures (900°C-1100°C) to close off the surface-connected porosity thereby encapsulating the radioactive gases in a chemically and mechanically durable waste form for long-term storage of ^{129}I, ^{85}Kr, and $^{14}CO_2$. High chemical durability and structural stability of the waste form is achievable with high silica and low modifier oxide contents. Moreover, silica glass exhibits good mechanical properties and thermal shock resistance.

Low-cost silica aerogels with surface areas of approximately 1250 m^2/g are commercially available from a variety of vendors. Their high surface areas are achieved at minimal cost because of the methods used for their synthesis. No time-consuming and expensive templating process is necessary for the manufacture of aerogels, as both the flash evaporation and supercritical fluid drying routes for their synthesis are readily amenable to large-scale production.

Chemical stability, non-flammability, large surface areas per unit volume, and high affinity and selectivity for specific targets make Ag-functionalized carbon aerogels the promising materials for removal of radionuclides from off-gas stream.

3.1.1 Silica Aerogel

A monolayer of selective functional groups may be created on the silica aerogel surface through the use of organosilanes (Fryxell et al. 2007). Thermogravimetric data obtained at PNNL indicate that the thermal decomposition temperature of many organosilane-modified silica structures in air to be above 175°C (Fryxell et al. 2007). The silica aerogel surface may be functionalized with silanes through the use of a tunable solvent, such as super-critical CO_2. Use of conventional solvents, especially protic ones, can

cause collapse of the pore structure from capillary forces exaggerated by hydrogen bonding with surface hydroxyl groups. Once the surface hydroxyl groups are capped with organosilanes, the aerogel structure is stabilized with respect to contact with liquids. Use of a supercritical solvent avoids pore collapse because it has negligible surface tension and facilitates high density surface coverage because of the gas-like diffusivity and efficient pore penetration of supercritical solvent.

3.1.1.1 Silica aerogel for iodine capture

Metallic and ionic silver are known to have a strong affinity for gaseous iodine species (Scheele, Burger, and Matsuzaki 1983; Scheele, and Burger 1987; Scheele, Burger, and Halko 1988). Silica aerogel surfaces coated with silver are expected to have high affinity and selectivity for iodine. These can be functionalized in super-critical CO_2 to form end members containing Ag (Figure 2)

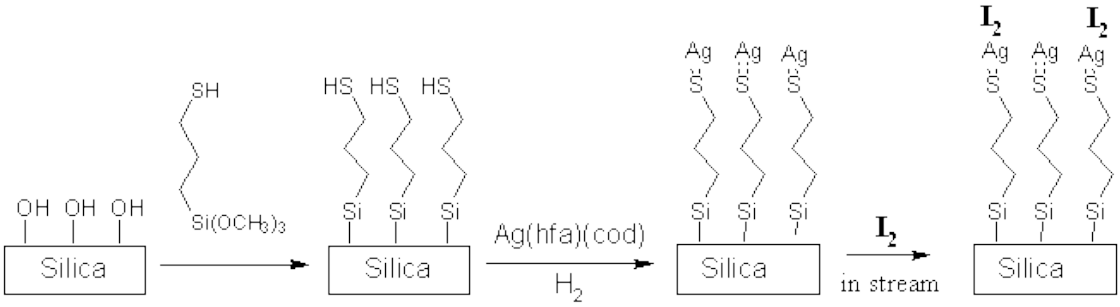

Figure 2. Schematic of Surface Functionalization of Silica Aerogel with Organic Thiol Groups

3.1.1.2 Silica aerogel for carbon dioxide capture

Amine groups are known to have a high affinity for CO_2 (Zheng et al. 2005). The strength of interaction between an amine-functionalized silica surface and a carbon dioxide gas stream can be controlled through selection of the amine for the surface modification. As above, these can be functionalized in super-critical CO_2 (e.g. Figure 3)

3.1.1.3 Silica aerogel for krypton capture

Though cryogenic temperatures are required for significant adsorption of krypton on silica, the affinity of silica for krypton can be increased through the addition of fluoroalkyl or perfluoroalkyl groups to the silica surface. Silica will be treated in a heated vessel with an organic silane in supercritical carbon dioxide to produce the monolayer. Excess silane and the methanol byproduct of the reaction will be removed from the aerogel by flushing with additional carbon dioxide followed by nitrogen. A typical example of this process is shown in Figure 4.

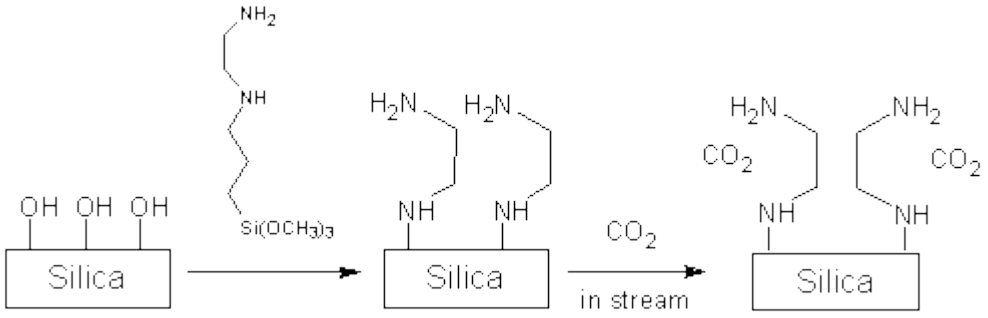

Figure 3. Schematic of Surface Functionalization of Silica Aerogel with Amine Groups.

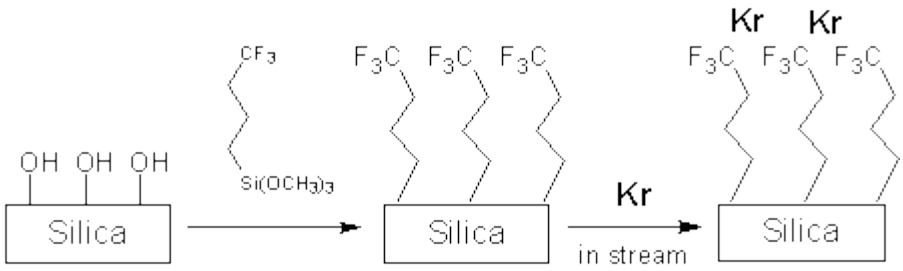

Figure 4. Schematic of Surface Functionalization of Silica Aerogel with Fluoroalkyl Groups.

3.1.1.4 Densification of silica aerogels

After use, the high surface area and porosity aerogels must be disposed. One approach for reducing the surface area and porosity with the subsequent reduction in radionuclide release is densification. Silica aerogels can be densified by thermal sintering at ~1050°C, isostatic compression at room temperature, or combination of both methods. The kinetics of thermal sintering is affected by the initial pore size distribution and the rate of densification can be accurately predicted from the theory of viscous sintering by Scherer et al(1998). The isostatic compression method uses mercury that cannot enter the small interconnected pores of the aerogel to partially densify the porous network of aerogel materials (Alaoui et al. 1998; Duffours, Woignier, and Phalippou 1995; Pirard et al. 1995; Scherer et al. 1995). The isostatic pressure mainly affects the largest pore size of the aerogel, while the specific surface area remains constant during compression (Dieudonne, and Phalippou 1999). This densification depends on structural properties of the aerogel and on the chemical nature of the surface under a given pressure of mercury (Perin et al. 2004). It was shown that isostatic compression followed by thermal sintering reduces considerably the time required for partial or full densification (Perin L. et al. 2003). The larger pores are transformed into numerous smaller pores, allowing acceleration of the thermal sintering processes.

The partial densification of silica aerogels will be achieved with isostatic compression of aerogels with a mercury porosimeter. The thermal sintering of the surface layers of porous aerogels will be achieved by performing a fast thermal treatment within a small temperature range (e.g. 1000-1100°C for silica aerogels) within which viscous flow sintering occurs. This rapid sintering will close the interconnected pore-channel network on the surface, but the remainder of the pores will stay interconnected. This approach will not be acceptable for the immobilization of radioactive waste because breakage of the sintered layer would expose the captured radionuclides to the ground water in the repository. Therefore, to isolate the pores, the thermal sintering of aerogels at longer times will be investigated. The critical porosity, at which the pore network will close lies between 4 and 10% for typical ceramics (Shaw 1998). In addition, we will investigate the use of hot isostatic pressing, a combination of high pressure and elevated temperature, to sinter aerogel materials through plastic deformation.

3.1.1.5 Chemical durability of sintered aerogels

Silica aerogels have been investigated by Woignier et al. (1998) for the storage of long life actinide wastes. The authors impregnated the porous aerogels with solutions of the “actinide salts” simulated by neodymium nitrate and, after removal of the liquid phase, the aerogels were sintered into a composite glassy material containing approximately 10 mass% of Nd_2O_3. Their experimental results indicated that the final product has a chemical durability that is two orders of magnitude better than that of borosilicate glass.

3.1.1.6 Mechanical durability of sintered aerogels

The compressive strength of aerogel-stabilized waste forms has not been adequately studied. However, the mechanical strength of a consolidated aerogel is expected to be as good as glass and exceed that required for disposal in a repository.

3.1.2 Carbon aerogels

Carbon aerogels are typically prepared through the sol-gel polymerization of resorcinol with formaldehyde in aqueous solution to produce organic gels that are then supercritically dried and subsequently pyrolyzed in an inert atmosphere (Berthon-Fabry et al. 2004; Brandt, and Fricke 2004; Pekala 1989; Pérez-Caballero et al. 2008; Wiener et al. 2004). Several possibilities exist for reducing the cost of producing carbon aerogels, including several new synthetic routes for preparation of organic aerogels. Pekala et al. (1995) developed a new type of organic aerogel based upon a phenolic-furfural reaction in alcohol. Wu et al. (2005) prepared organic aerogels from the sol-gel polymerization of cheap phenol with formaldehyde with NaOH as the base catalyst. Li et al. (2000) used reaction of cresol with formaldehyde also catalyzed with NaOH solution. Zhu et al. (2006) followed the same synthetic route as Li et al. but applied ambient pressure drying instead of supercritical drying, further reducing the cost of carbon aerogel.

3.1.2.1 Carbon Aerogels for iodine capture

To increase the affinity for iodine, the surface of a carbon aerogel may be doped with Ag. The selectivity of carbon aerogels may be controlled by covalent and noncovalent surface modification. A common method for covalent modification of a carbon surface is to first oxidize the surface to produce oxygen-containing reaction sites and then to couple selectivity-inducing functional groups to the surface through these reaction sites. An alternative method for covalent modification of carbon surfaces is the direct addition of chemical groups to carbon-carbon bonds through reactions such as diazonium coupling or 1, 2-dipolar addition, or by making inherently functional mesoporous carbons (Shin et al. 2007). Selectivity may also be noncovalently induced onto the carbon surface through the directed adsorption of molecules or particles containing selective functional groups. Silver-doped surface aerogel can be produced by decoration of silver nanoparticles onto the carbon surface (Figure 5), thereby giving iodine selectivity to the aerogel.

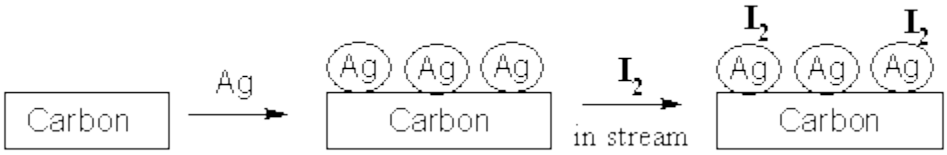

Figure 5. Schematic of Decoration of Silver Nanoparticles onto the Carbon Aerogel Surface.

4. Krypton-85

Because their chemistries are very similar, it is likely that any process to remove Kr is likely to also remove the Xe, since it is heavier and more reactive. Of these two elements, fission product Xe is much more abundant (Table 1) (Wanless, and Thode 1955). As all of the radioactive Xe isotopes are very short lived - ^{127}Xe has the longest half life at 36.4 d – and the storage time for SNF is longer than about 2 years (a reduction in the ^{127}Xe by at least 10^8), the radioactive Xe isotopes have all decayed to insignificant amounts by the time the fuel is processed. Therefore, the assumption is that all Xe is nonradioactive and, because of the similarity of chemistry, is immobilized along with the Kr.

Five technologies were proposed for the removal and immobilization of Kr and Xe: functionalized aerogels (previous section), silicon carbide, Li(Ag)-doped inorganic adsorbents, and functionalized multi-walled carbon nanoparticles.

4.1 Silicon Carbide for Immobilization

Because of the low diffusivities for fission products and superior physical and chemical stability of silicon

Table 1. Fission Product ratios of Krypton and Xenon isotopes from Irradiated U-235 Fuel.

Isotope	Atom %	Absolute fission yield (%)
Kr-83	14.10	0.557
Kr-84	12.93	1.02
Kr-85 (10.27 yr.)	7.59	0.300
Kr-86	52.38	2.07
Xe-131	13.42	2.93
Xe-132	20.08	4.38
Xe-134	36.91	8.06

carbide (SiC), it is an ideal candidate for immobilization of C, Kr, and Xe (and perhaps other fission products). Silicon carbide possesses excellent physical and chemical properties that make it a promising material, not only for advanced electronic devices (Raynaud 2001), but also for structural components in fusion reactors (Fenici et al. 1998; Nogami et al. 2009; Zhao et al. 2007; Wong et al. 2007; Katoh et al. 2007), a barrier for fission product diffusion in gas-cooled fission reactors (Kim et al. 2000), and an inert matrix for the transmutation of plutonium and other transuranics (Verrall, Vlajic, and Krstic 1999; Krstic, Vlajic, and Verrall 1996). The high thermal conductivity of SiC also enhances homogeneous heat distribution in devices and rapid heat transfer. Unlike traditional semiconductor materials, thermal diffusion of dopants in SiC requires extremely high temperatures because of the extremely low diffusivities for impurities in SiC. This low diffusivity for impurities is one of the reasons SiC is used as the fission product barrier in tristructural-isotropic (TRISO) nuclear fuel and its use for this application has been demonstrated at temperatures over 2000 K (Schenk, and Nabielek 1991; Schenk, Pott, and Nabielek 1990; Nabielek et al. 1990). Because of the low diffusivities for fission products and superior physical and chemical stability of SiC, it is an ideal candidate for immobilization of C, Kr, and Xe (and perhaps other fission products). Thermal release of helium generated in neutron-irradiated SiC does not occur until temperatures above 1200 K (Sasaki et al. 1991; Sasaki, Maruyama, and Iseki 1989). Because of its low chemical reactivity, SiC is also proposed as cladding for advanced light water reactors[a] (Filippov et al. 2007a; Filippov et al. 2007b; Filippov et al. 2006). A recent discovery of pitting corrosion in β-SiC at 300˚C, however, indicates that even this stable material is not immune to low-temperature corrosion involving volatile SiOH species (Henager Jr et al. 2008). Although pits were observed in this study no measurable mass loss occurred for exposure times up to 4000 hours. While oxidation of SiC occurs at elevated temperatures, such oxide films generally form a barrier to further oxidation and should be negligible under conditions for immobilization unless significant water vapor is present (Opila 2003). Silicon carbide also occurs in nature as the extremely rare mineral moissanite (Bauer, Fiala, and Hrichova 1963; Pierro et al. 2003), and SiC crystals of interstellar origin have been found in primitive meteorites (Alexander, Swan, and Walker 1990), both of which support its physical and chemical stability.

Since industrial scale fabrication of SiC monoliths with physical vapor deposition methods is a well-established technology (Abe et al. 2008; Jiangang et al. 2006; Saddow et al. 2001; Moon et al. 2001; Sugiyama et al. 1998), there is little, if any, technology development needed to produce dense, pure SiC. While there are many polymorphs of SiC, the cubic 3C structure is preferred for nuclear and structural applications, such as ceramic composite fibers and matrices and fine-grained coatings for TRISO nuclear fuel particles. Much of our knowledge of diffusivities of nuclear isotopes in SiC comes from studies of TRISO fuel particles (Peterson, and Dunzik-Gougar 2006; Schenk, Naoumidis, and Nickel 1984; Smith 1979; Fukuda, and Iwamoto 1978; Fukuda, and Iwamoto 1976; Fukuda, and Iwamoto 1975). Studies have shown that Xe and Kr have extremely low mobilities in SiC at low temperatures and only become mobile above 1200˚C (Fukuda, and Iwamoto 1978; Fukuda, and Iwamoto 1976; Fukuda, and Iwamoto 1975). Thus, it appears that SiC is almost an ideal candidate material for storage and retention of radioactive C, Xe, and Kr.

[a] http://findarticles.com/p/articles/mi_hb5260/is_200411/ai_n20368827/?tag=rel.res1; http://web.mit.edu/canes/publications/abstracts/nfc/nfc-098.html

For immobilization of fission products, physical vapor deposition of monolithic 3C-SiC provides an industrial scale process[b] from which to begin this development. We anticipate that some optimization of either PVD or CVD technology with ion-assisted deposition would be required in designing a process to entrain radioactive C, Xe, and Kr. Captured carbon from reprocessing could supplement the carbon source used in processing, typically in the form of methyltrichlorosilane, CH_3SiCl_3 (Jiangang et al. 2006). Gaseous fission products, such as Xe and Kr, could be injected onto the surface with low energy ion guns or leaked into processing chamber (Grigorov, and Martev 1988). The radioactive C would be incorporated directly into the SiC structure (see Section 2.0), while Xe and Kr would be incorporated interstitially, trapped at processing defects, or trapped in small bubbles that may form during processing. One prior study indicated that up to 20 atomic % Ar could be entrained during PVD of Ti-films (Grigorov, and Martev 1988). It is anticipated that equivalent amounts for Xe and Kr could be entrained within CVD or PVD SiC. Since Xe and Kr diffusivities are extremely low at ambient temperatures, the release rates of Xe and Kr are negligible, even along grain boundaries, for millions of years (Sauvage et al. 2007; Van Ginhoven et al. 2006; Pramono, Sasaki, and Yano 2004; Chen, Jung, and Trinkaus 2000; Jung 1992; Fukuda, and Iwamoto 1978; Fukuda, and Iwamoto 1976).

4.2 Krypton and Xenon Capture with Li(Ag)-Doped Inorganic Adsorbents

Radioactive off-gases from nuclear fuel reprocessing are released primarily in the head-end activities including fuel chopping and dissolution processes. In past practice, the volatile radionuclides (including Kr and Xe) were discharged to the environment through the off-gas system typically after scrubbing with sodium hydroxide to remove nitric oxides and filtering through special zeolites or charcoal to remove radioiodine. The current EPA standards for release of ^{85}Kr to the atmosphere from nuclear power operations have been established (EPA 2008). The total quantity of radioactive materials entering the environment from the entire uranium fuel cycle, per gigawatt-year of electrical energy produced by the fuel cycle contains less than 50 000 curies of ^{85}Kr, which will limit the free release ^{85}Kr in future processing plants.

Many processes have been proposed for Kr removal, including cryogenic distillation (Anderle, Frey, and Lerch 1977; Glatthaar 1976; Green, Goossens, and Marien 1986; Hunter et al. 1986; Munakata et al. 1999; Schiller 1977), membrane separations (Stern, and Wang 1980; van den Bergh et al. 2008), ion sputtering (McClenahan et al. 1986; Romer, Henrich, and Fritsch 1986), selective adsorption on charcoal (Adams, Browning, and Ackley 1959; Bernhard et al. 1984; Choppin, Liljenzin, and Rydberg 1996; Forster 1971; Juntgen et al. 1978; Munakata et al. 1999; Ringel, and Printz 1986; Schröde.Hj, Queiser, and Reim 1971) zeolites (Anson et al. 2008; Bourrelly, Maurin, and Llewellyn 2005; Horton-Garcia, Pavlovskaya, and Meersmann 2005; Ianovski et al. 2002; Jakubov, and Mainwaring 2002; Kitani et al. 1968; Lim et al. 2001; Munakata et al. 1999; Pence, and Paplawsky 1980; Pribylov, and Yakubov 1996; Schiller 1977; Treacy, and Foster 2009; Ustinov, Vashchenko, and Katal'nikova 2000; van den Bergh et al. 2008), and a combination of cryogenic trapping and molecular adsorption (Munakata et al. 2006; Schiller 1977).

[b] http://www.rohmhaas.com/wcm/products/product_detail.page?display-mode=tds&product=1122020&application=

Cryogenic distillation is promising but has the disadvantages of high operating costs and potential hazards with accumulation of ozone; current membrane technology is limited by throughput capacity (Ianovski et al. 2002). Adsorbent technology with activated charcoal is advantageous because of ease and reliability of operation and relatively low operating cost associated with deployment (Kitani et al. 1968), but it has limited use because of rapid energetic reactions between NO_x and O_2 with activated charcoal (Benedict 1981). Recent results have shown that some inorganic adsorbents, namely zeolites and silicotitanates, demonstrate a large absorption capacity for Kr, near-comparable to charcoal (Ianovski et al. 2002), and have the advantage of no safety concerns associated with exothermic reactions between the adsorbent and O_2 or NO_x as with charcoal. Mineral properties of zeolites and silicotitanates are of particular importance. Their alumino-silicate construction is extremely durable, chemically resistant to the high humidity, NO_x-containing off-gas, customizable to provide pore sizes to accommodate or exclude selected gases based on size (molecular sieves), not combustible, and resistant to radiation.

Studies of silver or lithium-loaded zeolites and silicotitanates have reported an increased affinity over non-modified parent materials for noble gas inclusion from the metal-noble gas interaction within the pore structure. The interaction of a positive metal center (Ag^+) and an electron-rich noble gas (Xe or Kr) can be described as a weak Lewis acid (metal)/base (noble gas) affinity. Although the general Lewis acid/base chemistry of metal-noble gas interaction as a basis for the selective gas separation has not been carefully explored to date, the available results suggest that inorganic sorbents can be successfully used for Kr/Xe capture. This partitioning of Xe and Kr from nuclear fuel reprocessing off-gas streams might be accomplished with metal-doped inorganic zeolites and silicotitanates that have been modified to incorporate metals known for rich Lewis acid interactions such as Li, Ag, and first row transition metals. We plan to dope selected metals into various zeolites having appropriate pore sizes at various loadings and test the resulting sorbents.

To test the Kr and Xe uptake, a chromatographic system will be used containing the adsorbents of interest. The gas composition will simulate a PUREX or UREX head-end and dissolver off-gas of the fuel reprocessing plant. The current fuel pretreatment (as envisioned within existing US plans for reprocessing) consists of a voloxidation sequence (volox), in which the uranium in spent fuel will be oxidized under an oxygen atmosphere at moderate temperatures (<600°C) to triuranium octaoxide (U_3O_8). The oxidation step of forming metal oxides from the U-metal or uranium dioxide (UO_2) fuel will release the bulk of the volatile and semi-volatile fission products (Xe, Kr, I_2, etc) from the fuel. The oxide formed in the volox process will then be dissolved in nitric acid for processing with the PUREX or UREX flow sheet.

The volox process is only partially efficient (~60%) at releasing noble gases from metal-oxide fuels, the remainding fission gas is released during the nitric acid dissolver stage, which requires the Kr/Xe trapping mechanism to be resistant to both voloxidation and dissolver off-gas streams. The voloxidation process produces less NO_x and water vapor than the nitric acid dissolution stage, simplifying the off-gas treatment requirements for that system stream. However, the complexities of competing adsorbent gases including NO_x, N_2, O_2, and water vapor need to be investigated. The proposed work includes identification of the best performing metal-substituted zeolites and titanosilicates for Kr/Xe capture and initial recommendation for the off-gas system design.

4.3 Carbon Nanotubes for Krypton Separation and Immobilization

4.3.1 Summary of Findings

Carbon nanotubes (CNTs) as adsorbents for Kr gas, in which the Kr is adsorbed to the outside of the carbon nanotubes, most likely will not offer significant improvement over proven zeolite adsorbents. Carbon nanotube membranes have great potential to provide a step-change improvement over existing gas separation membrane technology because of their unusually high molecular transport. However, it

remains unclear how a high selectivity for Kr can be achieved by controlling CNT structures or functionalization. Finally, encapsulation inside the CNTs does seem to offer opportunities to immobilize Kr gas in a unique stable solid form.

4.3.2 Gas Adsorption on CNTs

Different adsorption sites exist in CNTs: grooves on the outer surface of nanotube bundles, non-groove sites on the outer surface, interstitial channels between adjacent nanotubes, and interior channels. Extensive theoretical modeling and experimental measurements were done to understand adsorption of gas into these sites. A brief summary of literature dealt with Kr or other noble gas adsorption by CNTs is provided below.

Muris et al. (2000) were among the first to study Kr adsorption on single-walled carbon nanotubes (SWNTs) at 77.3 K. The SWNTs had closed ends. Thus, adsorption into the interstitial channels and on the outside of the SWNT bundles gave rise to stepwise isotherms. Talapatra et al. (2000) measured the adsorption isotherms of Xe from 220 to 295 K on closed-end SWNTs. They determined that the binding energy of Xe on SWNTs, 282 meV, is about 75% higher than that of Xe on planar graphite. Bougrine et al. (2002) reported Kr adsorption isotherms on multi-walled nanotubes (MWNTs) at 77 K. The nanotube samples they used were most likely close-ended. Later works shifted to open-ended nanotubes, particularly open-ended SWNTs, to access the interior cavity. Babaa et al. (2003) produced open-ended SWNTs by mechanical grinding followed by annealing at 600 °C under vacuum. They measured adsorption isotherms of Kr between 77 and 93 K and Xe between 110 and 120 K and attributed the increased adsorption at low relative pressure to filling of the internal channels. Similar experiments were done by Yoo et al. (2003) on N_2 adsorption from 71 to 130 K by open-ended SWNT bundles. Their nanotube samples were opened by treatment with a mixture of H_2SO_4 and HNO_3 and annealed at high temperature. Binding energy of N_2 with open-ended SWNTs was estimated to be 161 meV, compared to 78.5 meV for the closed-ended nanotubes. Thus, inner sites of the nanotubes were favored over interstitial channels and outer surfaces. Arab et al. (2006) later provided a method to estimate SWNTs opening ratio based on the difference of Kr or Xe adsorption on open- and closed-ended SWNTs. This was an extension of the earlier work by Babaa et al. (2003) Rawat et al. (2007) reported adsorption kinetics of Ar at 77 K on closed- and open-ended SWNTs. The nanotubes were opened with the standard acid treatment method. Jalili et al.(2007) studied Kr and Xe adsorption on open SWNTs using molecular dynamics simulation. The binding energies at low coverage were estimated to be 4.87 meV for Kr and 7.62 meV. These values seem too low.

Based on the literature reviewed, adsorption of Kr and Xe on both open- and closed-ended CNTs is a process of physical adsorption, i.e. nonspecific to the gases. A significant amount of adsorption is limited to low temperatures only. This does not offer any significant advantage of CNTs as adsorbents to capture Kr or Xe compared to conventional adsorbents, such as zeolite. Note that most of the data from experiments or MD simulations were for single gas components. While binding energies for some gas species were reported, a reliable comparison of those for Kr, Xe, and N_2 is not possible at this time due to a lack of data.

4.3.3 CNT Membranes

An alternative application of CNTs is to use the center pores inside CNTs as a unique environment for molecular transport. Recent theoretical studies have predicted that diffusivities of simple gas molecules inside the CNT pores are orders of magnitude higher than those in polymers and zeolites (Jakobtorweihen, Keil, and Smit 2006; Newsome, and Sholl 2006; Skoulidas, Sholl, and Johnson 2006; Whitby, and Quirke 2007). These pure gas diffusivity results have been confirmed in experimental studies (Hinds et al. 2004; Holt et al. 2006; Majumder, Chopra, and Hinds 2005). Some of the recent results were covered in two review articles (Noy et al. 2007; Whitby, and Quirke 2007). The fast transport inside CNTs was believed to be the result of the smooth potential-energy surface at the CNT

inner wall. These intriguing properties make it possible to design a CNT membrane that has intrinsically high permeability. While most of the current work on gas transport in CNTs focuses on pure gases, molecular simulations have also predicted selectivity of methane over hydrogen in SWNTs from selective adsorption (Chen, and Sholl 2006). Additionally, open ends of CNTs are easily functionalized, providing an additional way to impart selectivity through manipulation of the entrance resistance, i.e. gated channels (Majumder, Chopra, and Hinds 2005). Therefore, a CNT membrane has the potential to overcome the trade-off between high permeability and selectivity for conventional gas separation membranes.

The published methods of preparing CNT membranes fall into five categories: (1) impregnation of a dense array of CVD-grown aligned CNTs with polystryrene polymer (Chopra et al. 2007), (2) embedding a dense array of CVD-grown aligned CNTs in a rigid silicon nitride film (Holt et al. 2006), (3) self-assembly of cut CNTs with filtration in a support polymer membrane and subsequent sealing with a polymer (Kim et al. 2007), (4) collapse of an isolated dense array of CVD-grown CNTs by capillary forces in solvent evaporation (Yu et al. 2009), and (5) pyrolysis of carbon precursors in an anodic aluminum oxide template (as reviewed by Whitby and Quirke (2007)). Type 5 membranes typically contain more amorphous nanotubes and are mainly studied for liquid transport. Type 1-4 membranes are studied for gas transport. Type 4 membranes contain both CNT core channels and interstitial channels since the CNTs are not embedded by an impermeable matrix. All published CNT membrane permeance data show orders of magnitude higher values than Knudsen diffusion predictions, highlighting the fast molecular transport through CNTs. Single component gas selectivity generally exhibit Knudsen-like scaling, i.e. permeability scales with the inverse square root of gas molecular weight (Holt et al. 2006; Kim et al. 2007; Yu et al. 2009), although hydrocarbons exhibit higher selectivities on the silicon nitride embedded CNT membranes (Holt et al. 2006).

For the target application of separating Kr or Xe from waste air streams, a membrane-based process that is selective towards Kr/Xe can be very efficient, since only trace amount of these gases are present and need to permeate across the membrane. If only Knudsen diffusion dominates the selectivity, then a CNT membrane will not be selective towards Kr or Xe over N_2 or O_2 as the latter two gases are lighter in molecular weight. As demonstrated by MD simulation, entrance resistance also plays an important role in gas transport through CNT membranes (Newsome, and Sholl 2006). Non-Knudsen selectivity may be achieved by functionalizing the CNT pore entrance, but current literature offers clear direction as to how this may be done for the Kr/air separation pair.

4.3.4 Gas Encapsulation by CNTs

Encapsulation of molecules inside CNTs affects both the encapsulated molecules and the host CNT structure. There is currently much ongoing work that aims to understand the fundamental process and exploit it for gas sensors, biological sensors, nanoelectronics, and chemical reactions in confined environments. A recent article provides an excellent review of the field (Britz, and Khlobystov 2006). For long term storage of Kr gas, encapsulation in CNTs has the advantage of converting the waste form from gas to solid and reducing waste mobility. The key is how to infuse Kr gas into CNT inner pores and to block entrance for stable storage.

There is experimental evidence that CNTs are capable of confining high pressure gas. Gadd et al. (1997) provided an account of experiments to drive high pressure argon into MWNTs and showed with TEM analysis and x-ray spectroscopy that Ar was trapped inside the nanotubes. The internal pressure of Ar was estimated to be as high as 60 MPa. The filled tubes were found to retain the Ar with little change over several months at room temperature. The MWNTs had either a scroll or stacked cone structure with approximately 9° angle between the nanotube axis and the graphitic layers. The entrance of Ar into the nanotubes was suggested to be between the slanting graphitic layers that became permeable at the high temperature during gas loading (650°C and 170 MPa). An amorphous outer layer of carbon formed after

treatment was believed to have prevented gas from escaping. This method has the advantage that nanotube ends need not be opened and re-sealed for gas storage.

Matranga and Bockrath (2005) later developed a procedure to confine gases in SWNTs. Their method involves ozone treatment to open the nanotube ends followed by high temperature annealing. Gases were cryogenically adsorbed into the open SWNTs. A second low-temperature ozone treatment functionalized the entrance of SWNT pores, which created a steric barrier for keep trapped gas from escaping. Carbon dioxide and SF_6 were successfully trapped with this method. Only low pressure gas loading was demonstrated in this work. The steric blocking of CNT ends was air sensitive and loss of trapped gas occurred when sample was exposed to room air, probably due to hydrolysis of any ozonide blocks.

Another possibility to trap Kr inside CNTs is to blend Kr with precursor gases directly during the CVD synthesis of CNTs. This method is not reported in the literature. However, there are published papers on the analysis of the gas content of as-grown CNTs. The advantages of this method are that it is compatible with existing CVD technology and the Kr-containing CNTs can be produced with closed ends. One drawback is that the Kr loading may be limited by other carrier gases needed for the CVD synthesis.

4.3.5 Porous Metal-Organic Frameworks for Xe and Kr Storage

Like zeolites, organic and metal-organic frameworks (MOFs) consist of open frameworks that can accommodate several different gas species. Different than zeolites, MOFs represent a new class of functional materials consisting of metal centers linked with organic building blocks to produce diverse and customizable structural frameworks. These metal centers and organic linkers readily self-assemble into materials with open framework structures, where all the porosity is accessible for gas storage, separation and catalysis applications (Rowsell et al. 2005). Several porous materials (zeolites, activated carbons) were reported for gas storage applications but MOFs have received considerable attention over the past few years because of the high mass flux, thermal stability (in excess of 500°C for some MOFs), adjustable chemical functionalities and pore sizes, extra high porosity, and availability of hundreds of well characterized materials reminiscent to zeolites (Thallapally et al. 2008). In addition, they readily grow as crystals of a different sizes suitable for gas separation (e.g. to ca. 100 micrometre-size particles).

One of the methods most used to design and synthesize MOFs is to combine transition metal cations and multidentate ligands such as carboxylates to consistently arrive at more rigid networks. Figure 6 shows schematically a few MOFs that were generated from zinc nitrate and various organic pillars to consistently arrive more rigid frameworks with adjustable pore sizes. These materials have found great promise for the sequestration of CO_2. For example, Yaghi and co-workers (Millward, and Yaghi 2005) have shown that metal-organic framework-177 (MOF-177) exhibits a CO_2 sorption capacity of 1.4 g of CO_2 per gram of sorbent material. This is a significant improvement over commercially available zeolite sorbents.

Although research to date is somewhat limited with regard to the noble gases, storage and separation of noble gases has been demonstrated with these sorbents. A porous MOF-filled container stores substantially more Xe or Kr than the same container without any sorbent as shown in compression curves of Figure 7 (Mueller et al. 2006). For the Cu-MOF studied, the capacity for Xe was twice that of a high surface area carbon (Ceca, AC-40 2000 m_2/g). In addition, properties for separating Xe and Kr have been demonstrated. The gas diffusion in a MOF is 2-3 orders higher than in high performance carbons and molecular sieves. This should lead to superior performance with greater speed and reduced energy consumption in technological applications, but the thermophysical properties of these materials with trapped noble gases were not examined. It is also possible to increase the uptake of Kr and other noble gases with higher surface area materials that have recently been reported (Thallapally et al. 2008; Férey et al. 2005).

These materials could augment the existing technology for the removal and disposal of Kr and Xe. One of the main concerns with storage of cryogenically separated Kr in stainless steel canisters at elevated pressures (the baseline approach) is the Rb that is formed as the ^{85}Kr decays. The use of MOFs augments this technology in two ways. First, it allows more gas to be stored in the canister (Figure 7) at lower pressures. Secondly, the decay product Rb would be isolated from the metal canister, since it would be in the MOF structure. In fact, any of the proposed technologies, with which Kr and Xe are separated and the separation material does not also serve as the waste form, would benefit from this technology because the storage pressure could be decreased and the quantity of stored Xe and Kr per unit volume increased.

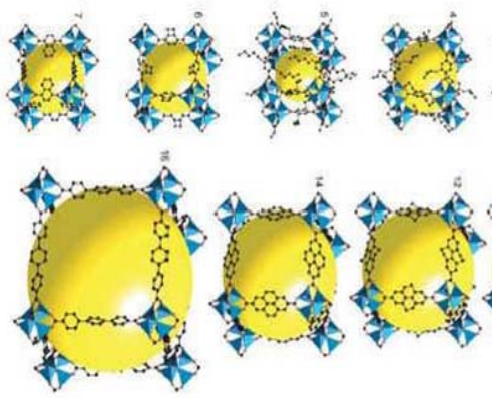

Figure 6. Metal-organic frameworks with different pore diameters.

5. Technology Selection

As stated in the Introduction, the number of technologies discussed above needs to be reduced to focus initial laboratory studies on the most promising candidates. An initial cut at making a short list of technologies to be investigated was carried out by the authors and an internal committee at PNNL.

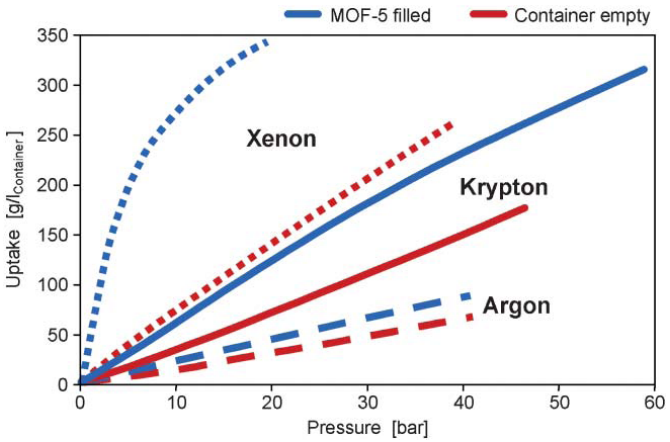

Figure 7. Comparison of Xe, Kr, and Ar uptake in cylinder filled with MOF-5 and an empty cylinder.

Of the technologies discussed above and in similar applications, there has been industrial experience with silicon carbide (large and complex structures are routinely manufactured; nuclear fuel applications show immobilization advantages), aerogels (manufacture of ceramic parts), amino-sorbent biomaterials, and porous metal-organic framework materials (CO_2 removal from operating coal-fired plants). Functionalized aerogels, Li(Ag)-doped inorganic adsorbents, carbon nanotubes, and porous metal-organic framework materials are proposed for removal of the target gas(es) and immobilization. These, then, minimized the number of unit operations in an operating plant.

The four technologies selected for initial testing are, in no particular order, silicon carbide, functionalized aerogels, carbon nanotubes, and porous metal-organic frameworks.

6. Summary of FY 2009 Progress

6.1 Hybrid Organic – Inorganic Solid Sorbents for Xe and Kr Immobilization

P. Thallapally

Initial tests of hybrid organic-inorganic solid sorbents were performed. The goal of this study was to demonstrate an ability to synthesize the materials, to establish that they had appropriately high surface areas, and to perform preliminary measurements of Kr absorptivity.

6.1.1 Synthesis and characterization

Benzene 1,4-dicarboxylic acid (30mg, Aldrich) and zinc nitrate hexahydrate (300 mg, Aldrich) were dissolved in 10 mL of *N*,*N*-dimethylformamide with stirring in a 20 mL vial and tightly capped and placed in a oven at 110°C for 20 h to yield MOF-5 crystals. After decanting the hot mother liquor the product was washed with DMF and dried in air for several hours. To produce the porous form of MOF-5, the resulting material was soaked overnight in 20 ml of methanol solution for at least 2-3 times in 3 days to replace the trapped DMF molecules. The trapped methanol was removed at high temperature under vacuum to get a porous MOF-5. The simulated and experimental PXRDs of MOF-5 are identical and confirm the successful synthesis of MOF-5. Single crystal X-ray measurements of MOF-5 shows four Zn atoms are connected to six terephalic acid ligands in an octahedral fashion. The repetition of the same in three dimensions results in a cubic network structure filled with the solvent DMF molecules (Figure 8).

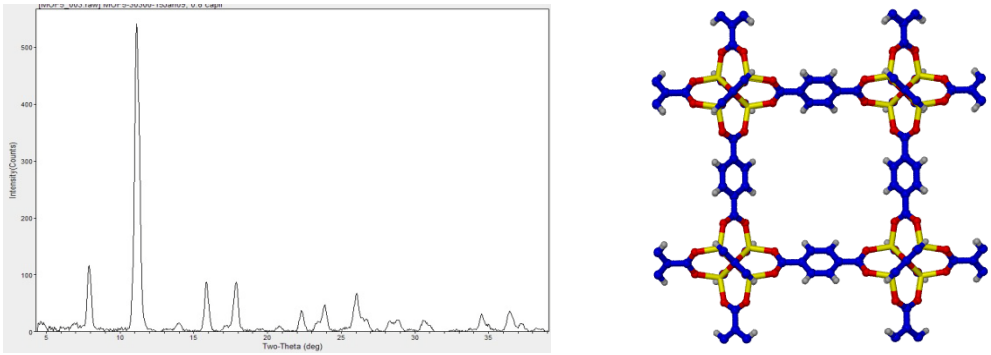

Figure 8. Powder X-ray and single crystal X-ray diffraction experiments confirms the successful synthesis of MOF-5. The solvent molecules were removed for clarity (right).

Thermogravimetric analysis of the resulting solid shows the mass loss of 5% between room temperature and 250°C that corresponds to the loss of trapped methanol molecules from the host lattice. No further mass loss was observed beyond 250°C, which shows the high-thermal stability of the compound. In order to confirm the porosity of the synthesized material BET surface area measurements on MOF-5 at 77 K and 100 kPa of nitrogen pressure was measured. The BET surface area of MOF-5 shows a typical type I isotherm with 1200 m^2/g of surface area, which is lower than the reported MOF-5. It is possible that the materials were not activated fully before the experiments were performed. Therefore, experiments are in progress to measure the accurate surface area of the material at identical conditions (Figure 9).

In a separate experiment, Kr sorption with a volumetric gas analyzer was conducted on a closely related analogue of MOF-5 after activating the synthesized material at 250°C overnight. Krypton gas was dosed every 5 minutes and amount of gas sorbed was calculated at each pressure. At about 20 kPa pressure, the material sorbs 8 mass% of Kr (Figure 10). Sorption experiments and other characterization are in progress on this material.

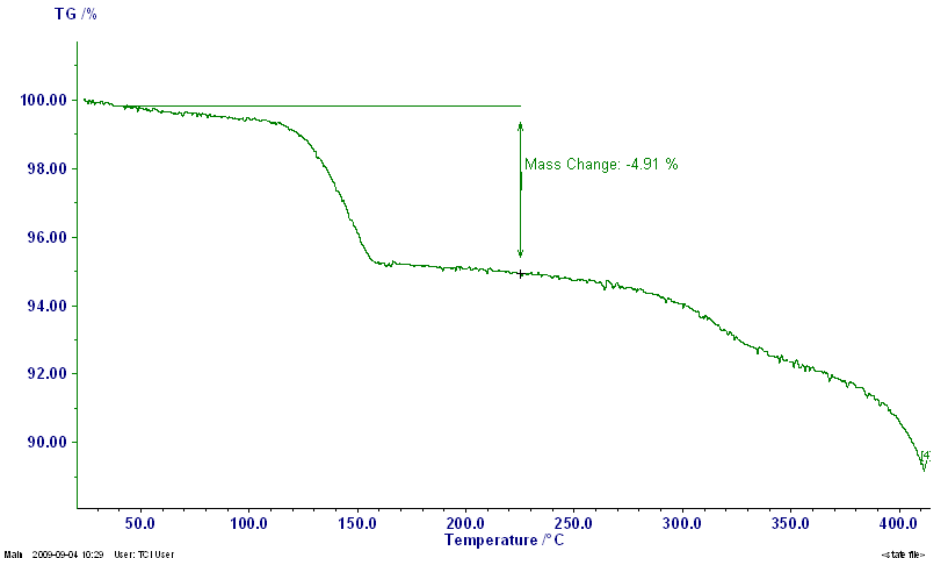

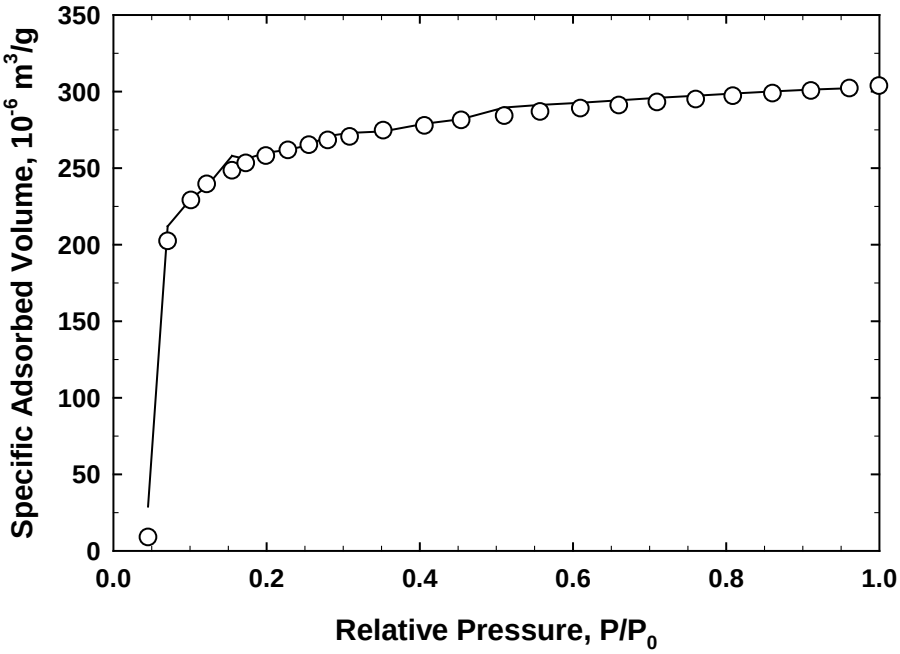

Figure 9. Thermogravimetric and BET surface area measurements of MOF-5.

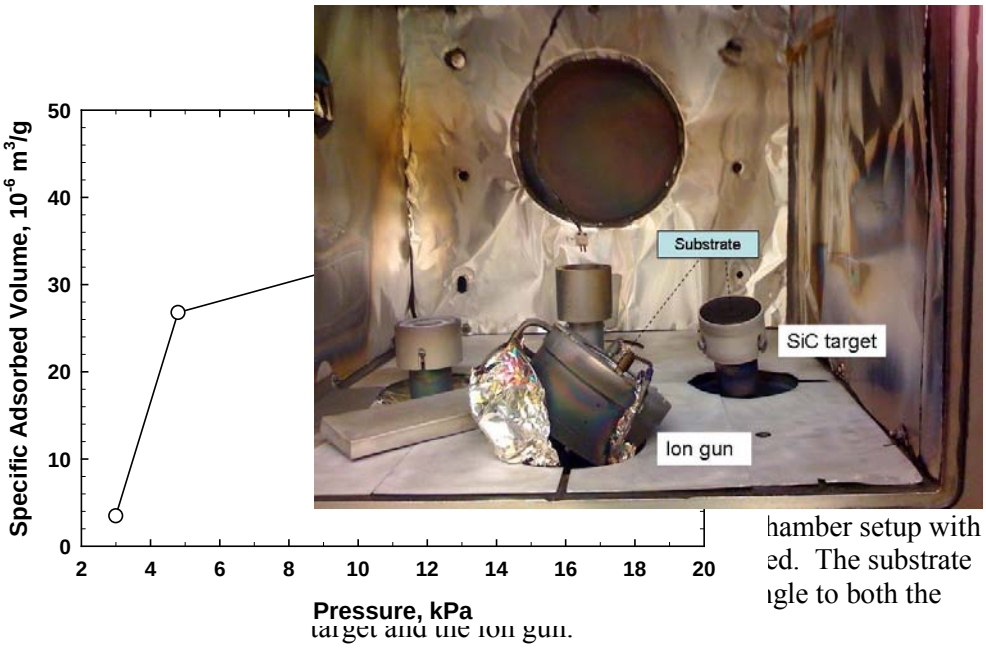

hamber setup with
ed. The substrate
ıgle to both the
target and the ion gun.

Figure 10. Krypton uptake at room temperature and 0.2 bar pressure with a volumetric gas analyzer.

6.1.2 Conclusions

The results from the work carried out in FY 2009 show that the MOFs are readily made and have high surface areas. Preliminary experiments with MOF-5 show that 8 mass% Kr can be sorbed at a moderate pressure of 20 kPa.

6.2 Immobilization of ^{85}Kr in SiC

C. Henager

It has been shown (see Section 4.1) that SiC has low release rates for He, with thermal release only occurring at temperatures above 1573K (1300˚C), we are studying the ability to store ^{85}Kr in SiC during sputter deposition in argon-krypton gas mixtures with and without ion-assisted deposition.
We have performed calibration runs to determine the SiC deposition rate using a bonded SiC target, with and without ion assist. The initial setup consists of the SiC target/cathode installed at a 20° angle toward the ion gun and the ion gun installed at a 35° angle toward the SiC target (Figure 11). One set of calibrations was done with the substrate positioned between the ion gun and target; the second set of calibrations had the substrate positioned closer toward the target. The goal of the calibrations was to determine the substrate positioning that gave us the most uniform and highest deposition rate. Argon and krypton (50%) gas were both fed through ion gun. Table 2 contains the deposition parameters for the calibrations (1A-S to 1D-S) and deliverable run (1E-S).

The low SiC deposition rates caused us to reconfigure the chamber to increase the SiC deposition rates. Figure 12 shows the general, not actual, setup used for a previous project. Cathode height and ion gun angle to be refined. Cathode is not tilted and the substrate can be positioned closer to increase the SiC deposition rate. The ion gun will be positioned similarly in relation to the cathode, but angled toward the lower substrate position that we will utilize. As before, all gases are introduced through ion gun.

At the time this report was written, experiments were underway to complete runs with a 1 μm SiC target, 100% Ar, 1 μm ion-assist SiC, 100% Kr on Si wafer, 2 μm SiC, 100% Ar on Si wafer, and 2 μm SiC, 100% Kr on Si wafer. These experiments were expected to be completed by September 30.

6.2.1 Conclusions

Delivery of materials and alteration of equipment resulted in delays in the experiments until after this report was submitted. However, SiC, because of the demonstrated low diffusion of lighter noble gases, is an excellent candidate for the immobilization of ^{85}Kr and by extension $^{129}I_2$.

6.3 Silica Aerogels: Novel Alternative Materials to Capture and Immobilize Gaseous Waste Streams of ^{129}I, ^{85}Kr, and $^{14}CO_2$

J. Matyáš, G. E. Fryxell, K. Wallace, and L. Fifield

6.3.1 Introduction

The objective of this project was to obtain proof-of-concept data on the ability of functionalized silica aerogel materials to capture and store ^{129}I, ^{85}Kr, and $^{14}CO_2$. To expedite the work, commercially available silica aerogel materials from United Nuclear were used. The surfaces of free-standing aerogels were chemically modified with the supercritical fluid chemistry previously developed at PNNL (US Patent #7,019,037 2006). This procedure is both fast and efficient and produces very little waste. The completeness of surface functionalization of aerogels was measured with Brunauer–Emmitt–Teller (BET) analysis and by thermogravimetric analysis - differential thermal analysis (TGA-DTA). The raw and iodine-loaded aerogels were densified thermally. In addition, the retention of iodine in sintered aerogels was quantified.

6.3.2 Chemical Modifications of silica aerogel surfaces

The silica aerogel surfaces were decorated with silver, an amine-containing monolayer, and alkyl-containing monolayer to create affinity and selectivity, respectively, for I, CO_2, and Kr.

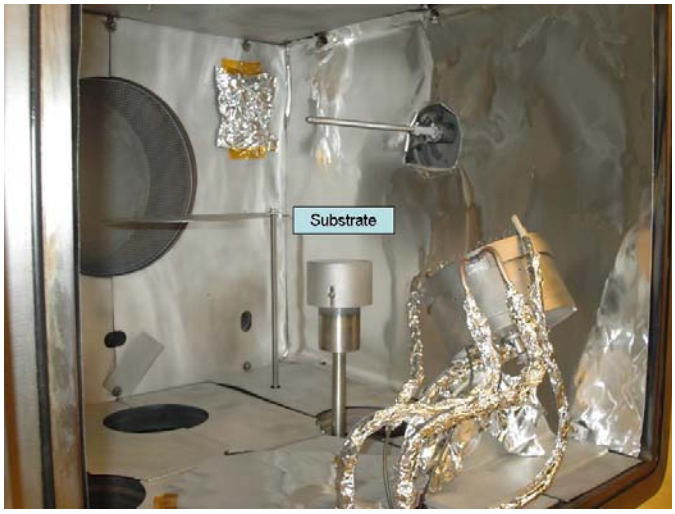

Figure 12. Reconfigured setup for SiC sputtering with ion-assist with normal incident angle for target to substrate to increase SiC deposition rates.

Table 2. Deposition Parameters

	System Parameters			Ion Gun Parameters				Cathode Parameters		Run			
	Pressure	Flow (SCCM)		Neutralizer		Drive		RF Power		Time	Rate	Substrate	
Run #	mTorr	Ar	Kr	Amp	Volts	kW	V	Watt	Voltage	min	A/min	Position	Comment
1A-S	4	37						205	123	235	23.3	center	Ar only calibration
1B-S	4	36						205	131	120	35	toward cathode	Reduced gap between substrate and cathode, Ar only calibration
1C-S	4	36		11.5	17.9	0.05	107	205	82	120	32.5	toward cathode	ion assist, Ar only calibration
1D-S	4	36		10.4	17.4	0.05	113	205	64	150	34.6	center	ion assist, Ar only calibration
1E-S	4	36						205	125	429	23.3	center	1 um goal: SiC: Ar only
1E-S	4.5	18	18	10.3	19.9	0.05	119	205	80	578	34.6	center	2 um goal: ion assist SiC : Ar/Kr

6.3.2.1 *Silica aerogel to capture and immobilize iodine*

The formation of silver nanoparticles on silica aerogel surfaces is schematically described in Figure 2 (Section 3.1.1.1). The hydrated granules of silica aerogel were functionalized with a mercaptan in supercritical CO_2. A 50% increase in mass suggested that more than half of the aerogel surfaces were coated with the mercaptan. Also, the comparison of BET surface area 737 m^2/g and pore volume 2.9×10^{-3} m^3/g with surface area 818 m^2/g and pore volume 5.4×10^{-3} m^3/g of raw aerogel confirmed uptake. A layer of Ag(I) was placed on the surfaces by reaction of the loaded aerogel with a $AgNO_3$ solution. The BET surface area of 986 m^2/g and pore volume 1×10^{-3} m^3/g indicated that the Ag(I) was taken up. After heat treatment, the Ag-impregnated aerogel sample (14847-8A-Ag-NP) had a surface area of 706 m^2/g and a pore volume of 7.0×10^{-4} m^3/g. The pore size distribution ranged from about 1.5 nm to 6.5 nm. The desorption pore size was very sharp (i.e. monodisperse) at 3.8 nm.

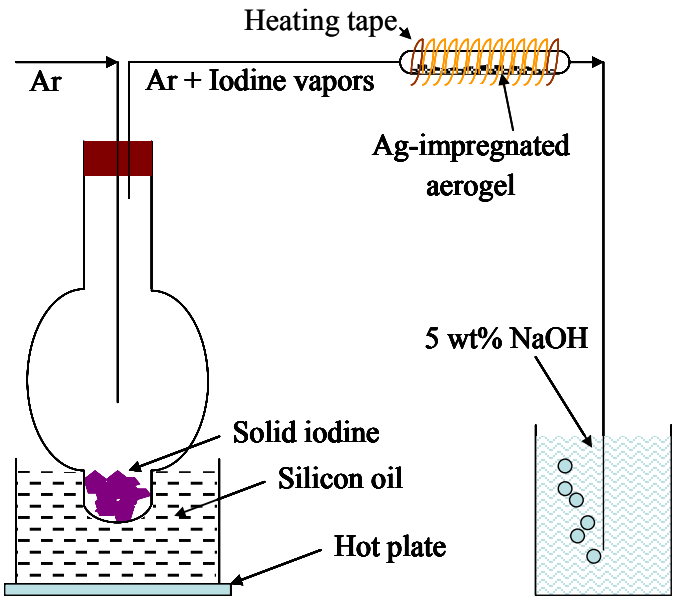

Figure 13. A schematic of the experimental apparatus to study the iodine absorption on silver impregnated silica aerogels.

6.3.2.2 *Silica aerogel to capture and immobilize krypton*

The functionalization of silica aerogel surfaces is schematically described in Figure 3. The hydrated granules of silica aerogel were functionalized through the creation of a monolayer on the surface by treating the aerogel in supercritical CO_2**.** However, the very limited change in mass, surface area, and pore volume suggest a lack of surface coating for the sample (KW-14847-9).

6.3.2.3 *Silica aerogel to capture and immobilize carbon dioxide*

The formation of amine monolayer on silica aerogel surfaces is schematically described in Figure 4. The hydrated granules of silica aerogel were functionalized through the creation of an amine monolayer on the surface by treating the aerogel with an organic silane in supercritical propane. A BET surface area 701 m^2/g and pore volume 2.4×10^{-3} m^3/g indicated a moderate coating of aerogel surfaces.

6.3.3 Gas uptake testing of chemically modified silica aerogels

The experimental setups for gas uptake testing of chemically modified silica aerogels and determined sorption capacities for iodine, krypton, and carbon dioxide are briefly described below.

6.3.3.1 *Iodine*

Figure 13 shows a schematic of the experimental apparatus that was designed and assembled to study the iodine absorption on silver impregnated silica aerogels. Approximately 5 g of solid iodine was heated to 85°C with a silicone oil bath. The subliming iodine was transported with ~20 mL/min of Ar flow through the heated ampoule containing ~0.5 g of Ag-impregnated aerogel, which was heated to ~115°C. The experiment lasted 24 h, after which the ampoule was removed and placed a vacuum desiccator for 30 min. It was then weighed. Two iodine gas sorption tests were run and their results are summarized in Table 1.

The high sorption capacity of Ag-impregnated aerogel in the test #1 was confirmed by chemical analysis (ICP-MS) and TGA-DTA.

6.3.3.2 Krypton

An experimental setup similar to that shown in Figure 13 that was designed and assembled to study the absorption of krypton on functionalized silica aerogels at room temperature (RT). The krypton gas was purged through glass ampoule with ~0.1 g of functionalized aerogel at flow rate of 5.5 mL/min to the beaker full of silicone oil. After 2 hours, the ampoule with sample was removed**,** put in a vacuum desiccator for 30 min and weighed. Two krypton gas sorption tests were run at room temperature with the results of 10.2 and 11.6 mg Kr/g. It is anticipated that more effective coating of the aerogel would lead to higher sorption capacity.

6.3.3.3 Carbon dioxide

The experimental setup similar to that shown in Figure 13 was used to study the absorption of CO_2 on amine functionalized silica aerogels at room temperature. A glass ampoule with ~ 200-mg aerogel was placed in an oven at 120°C for 30 min to drive off ambient CO_2 previously absorbed from the air. Next, the ampoule with sample was removed from the oven, put in the vacuum desiccators for 30 min, weighed (mstart), and purged with ~20 mL/min of CO2. After 2 hours, the ampoule with sample was placed again into the vacuum desiccator for 30 min and weighed (mend). Two carbon dioxide gas sorption tests were run at room temperature with the results of 16.8 and 18.7 mg CO2/g. In addition, the TGA-DTA was used to study the absorption and desorption of CO2 at higher temperatures. Approximately 20-mg sample was cycled between 120°C and 40, 60, 80°C with cooling and heating rates 5°C/min and 30 min dwell times at each temperature. These results indicated that the sorption capacity of the functionalized silica aerogels decreased with increasing temperature. The average sorption capacities at 40, 60, and 80°C were 14.8, 8.8, and 4.5 mg CO_2/g, respectively.

6.3.4 Immobilization of iodine-loaded silica aerogel

Figure 16 shows the experimental setup to effectively encapsulate the iodine gas in durable silica glass matrix through thermal sintering with pressure assistance. Approximately 0.5 g of sample was sintered in an alumina crucible at 1200°C for 30 min. The sample was removed from the crucible and analyzed for iodine with ICP-MS. The concentration of iodine in the glass sample was 142.2 mg I_2/g. Since the concentration of iodine in the iodine-loaded aerogel before sintering was 154.2 mg I_2/g, we were able to retain 92% of iodine in the final product (shown in Figure 17).

Table 1. Sorption capacity of Ag-impregnated aerogel for iodine.

Test #	Sorption capacity, mg I_2/g		
1	170.6[a]	154.2[b]	152.6[c]
2	196.0 [a]	N/A	N/A

[a] Obtained with weighing method (mass gain); [b] Obtained with ICP-MS;
[c] Obtained with TGA-DTA.

6.3.5 Conclusions

This work has shown that it is possible to functionalize aerogels despite the frailty of the aerogel backbone that these functionalized aerogels can be effective for capturing a variety of airborne target species, and that once laden with contaminants these materials can be sintered/densified, creating a stable composite that could be a viable waste form. We have demonstrated that Ag-impregnated silica aerogels are capable of efficient capture and sequestration of gaseous iodine. The functionalized aerogels exhibited high sorption capacity for iodine up to ~200 mg I_2/g at 115°C and retained 92% of iodine after thermal sintering with pressure assistance at 1200°C.

In spite of the poor coating of the silica aerogel, the functionalized material still demonstrated a sorption capacity of up to ~12 mg Kr/ g at room temperature. This is promising considering this value was obtained after the Kr-loaded aerogel was subjected to a low vacuum for 30 min. This suggests that Kr is reasonably retrained by the coating because the vacuum should have been sufficient to remove all the physically sorbed Kr.

The sorption capacity for CO_2 on functionalized silica aerogels was up to 19 mg CO_2/g at room temperature and decreased with increasing temperature.

In the course of these successful proof-of-concept experiments, we have learned that silica aerogels behave differently with the different coating chemistries and, while we were able to successfully functionalize these aerogels, the level of coating we achieved was lower than expected. Therefore, we feel that with optimization we could significantly improve the capture efficiencies for all tested gases.

This successful proof-of-concept research will result in invention disclosure.

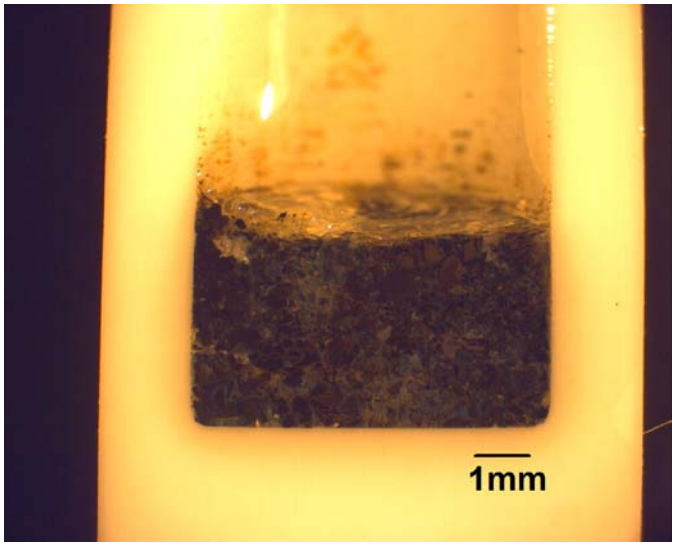

Figure 14. Iodine-loaded silica aerogel after thermal sintering at 1200°C for 30 min.

7. Bibliography

Abe, K, Y Nagasaka, T Kida, T Yamakami, R Hayashibe, and K Kamimura. 2008, "Characterization of Polycrystalline SiC Films Grown by HW-Cvd Using Silicon Tetrafluoride." Thin Solid Films 516:637-40.

Adams, RE, WE Browning, and RD Ackley. 1959, "Containment of Radioactive Fission Gases by Dynamic Adsorption." Industrial and Engineering Chemistry 51:1467-70.

Alaoui, AH, T Woignier, J Phalippou, and GW Scherer. 1998, "Room Temperature Densification of Aerogel by Isostatic Compression." Journal of Sol-Gel Science and Technology 13:365-69.

Alexander, CMOD, P Swan, and RM Walker. 1990, "In Situ Measurement of Interstellar Silicon Carbide in Two CM Chondrite Meteorites." Nature 348:715-17.

Anderle, F, H Frey, and G Lerch. 1977, "Cryogenic Recovery-System for Removal of Krypton 85 and Xenon 133 from Gaseous Wastes of Nuclear-Plants." Kerntechnik 19:483-87.

Anson, A, SM Kuznicki, T Kuznicki, T Haastrup, Y Wang, CCH Lin, JA Sawada, EM Eyring, and D Hunter. 2008, "Adsorption of Argon, Oxygen, and Nitrogen on Silver Exchanged Ets-10 Molecular Sieve." Microporous and Mesoporous Materials 109:577-80.

Arab, M, F Picaud, C Ramseyer, MR Babaa, F Valsaque, and E McRae. 2006, "Determination of the Single Wall Carbon Nanotube Opening Ratio by Means of Rare Gas Adsorption." Chemical Physics Letters 423:183-86.

Babaa, MR, I Stepanek, K Masenelli-Varlot, N Dupont-Pavlovsky, E McRae, and P Bernier. 2003, "Opening of Single-Walled Carbon Nanotubes: Evidence Given by Krypton and Xenon Adsorption." Surface Science 531:86-92.

Bauer, J, J Fiala, and R Hrichova. 1963, "Natural -Silicon Carbide." American Mineralogist 48:620-34.

Bernhard, G, W Bössert, O Hladik, and R Schwarzbach. 1984, "Chemical Reprocessing of Short-Period Irradiated Nuclear-Fuel for the Purpose of Producing Radioactive Isotopes (Die Chemishe Aufarbeitung von Kurzzeitig Bestrahltem Kernbrennstoff Für Die Gewinnung Radioaktiver Isotope)." Kernenergie 27:163-66.

Berthon-Fabry, S, D Langohr, P Achard, D Charrier, D Djurado, and F Ehrburger-Dolle. 2004, "Anisotropic High-Surface-Area Carbon Aerogels." pp. 136-44.

Bougrine, A, N Dupont-Pavlovsky, J Ghanbaja, D Billaud, and F Beguin. 2002, "Adsorption Studies of a Krypton Film Adsorbed on Catalytically Synthesized Multiwalled Carbon Nanotubes - Dependence on the Nanotube Morphology." Surface Science 506:137-44.

Bourrelly, S, G Maurin, and PL Llewellyn. 2005, "Adsorption Microcalorimetry of Methane and Carbon Dioxide on Various Zeolites." eds. J Cejka, N Zilkova and P Nachtigall, pp. 1121-28.

Brandt, R, and J Fricke. 2004, "Acetic-Acid-Catalyzed and Subcritically Dried Carbon Aerogels with a Nanometer-Sized Structure and a Wide Density Range." pp. 131-35.

Britz, DA, and AN Khlobystov. 2006, "Noncovalent Interactions of Molecules with Single Walled Carbon Nanotubes." Chemical Society Reviews 35:637-59.

Skoulidas, AI, DS Sholl, and JK Johnson. 2006, "Adsorption and Diffusion of Carbon Dioxide and Nitrogen through Single-Walled Carbon Nanotube Membranes." Journal of Chemical Physics 124.

Smith, CL. 1979, "SiC-Fission Product Reactions in Htgr TRISO Uc2 and Ucxoy Fissile Fuel. II. Reactions under Isothermal Conditions." Journal of the American Ceramic Society 62:607-13.

Stern, SA, and SC Wang. 1980, "Permeation Cascades for the Separation of Krypton and Xenon from Nuclear-Reactor Atmospheres." Aiche Journal 26:891-901.

Sugiyama, N, A Okamoto, K Okumura, T Tani, and N Kamiya. 1998, "Step Structures and Dislocations of SiC Single Crystals Grown by Modified Lely Method." Journal of Crystal Growth 191:84-91.

Talapatra, S, AZ Zambano, SE Weber, and AD Migone. 2000, "Gases Do Not Adsorb on the Interstitial Channels of Closed-Ended Single-Walled Carbon Nanotube Bundles." Physical Review Letters 85:138-41.

Thallapally, PK, J Tian, MR Kishan, CA Fernandez, SJ Dalgarno, PB McGrail, JE Warren, and JL Atwood. 2008, "Flexible (Breathing) Interpenetrated Metal-Organic Frameworks for CO2 Separation Applications." Journal of the American Chemical Society 130:16842-+.

Treacy, MMJ, and MD Foster. 2009, "Packing Sticky Hard Spheres into Rigid Zeolite Frameworks." Microporous and Mesoporous Materials 118:106-14.

Ustinov, EA, LA Vashchenko, and VV Katal'nikova. 2000, "Statistical Thermodynamics of the Adsorption of a Mixture of Krypton and Xenon on Zeolite Nax in the Approximation of an Ideal Adsorption Solution." Russian Journal of Physical Chemistry 74:1675-80.

van den Bergh, J, W Zhu, J Gascon, JA Moulijn, and F Kapteijn. 2008, "Separation and Permeation Characteristics of a Dd3r Zeolite Membrane." Journal of Membrane Science 316:35-45.

Van Ginhoven, RM, A Chartier, C Meis, WJ Weber, and LR Corrales. 2006, "Theoretical Study of Helium Insertion and Diffusion in 3c-SiC." Journal of Nuclear Materials 348:51-59.

Verrall, RA, MD Vlajic, and VD Krstic. 1999, "Silicon Carbide as an Inert-Matrix for a Thermal Reactor Fuel." Journal of Nuclear Materials 274:54-60.

Wanless, RK, and HG Thode. 1955, "The Fission Yields of Isotopes of Xenon and Krypton in the Neutron Fission of U-235 and U-238." Canadian Journal of Physics 33:541-54.

Whitby, M, and N Quirke. 2007, "Fluid Flow in Carbon Nanotubes and Nanopipes." Nature Nanotechnology 2:87-94.

Wiener, M, G Reichenauer, T Scherb, and J Fricke. 2004, "Accelerating the Synthesis of Carbon Aerogel Precursors." pp. 126-30.

Woignier, T, J Reynes, J Phalippou, JL Dussossoy, and N Jacquet-Francillon. 1998, "Sintered Silica Aerogel: A Host Matrix for Long Life Nuclear Wastes." pp. 353-57.

Wong, CPC, V Chernov, A Kimura, Y Katoh, N Morley, T Muroga, KW Song, YC Wu, and M Zmitko. 2007, "Iter-Test Blanket Module Functional Materials." Journal of Nuclear Materials 367-370:1287-92.

Wu, DC, RW Fu, ZQ Sun, and ZQ Yu. 2005, "Low-Density Organic and Carbon Aerogels from the Sol-Gel Polymerization of Phenol with Formaldehyde." Journal of Non-Crystalline Solids 351:915-21.

Yoo, D, G Rue, MHW Chan, Y Hwang, and H Kim. 2003, "Study of Nitrogen Adsorbed on Open-Ended Nanotube Bundles." Journal of Physical Chemistry B 107:1540-42.

Yu, M, HH Funke, JL Falconer, and RD Noble. 2009, "High Density, Vertically-Aligned Carbon Nanotube Membranes." Nano Letters 9:225-29.

Zemanian, TS, GE Fryxell, J Liu, S Mattigod, JA Franz, and ZM Nie. 2001, "Deposition of Self-Assembled Monolayers in Mesoporous Silica from Supercritical Fluids." Langmuir 17:8172-77.

Zemanian, TS, GE Fryxell, and OA Ustyugov. 2006, "Monolayer Coated Aerogels and Method of Making." US 7,019,037.

Zhao, J, G Wang, Q Guo, and L Liu. 2007, "Microstructure and Property of SiC Coating for Carbon Materials." Fusion Engineering and Design 82:363-68.

Zheng, F, DN Tran, BJ Busche, GE Fryxell, RS Addleman, TS Zemanian, and CL Aardahl. 2005, "Ethylenediamine-Modified Sba-15 as Regenerable CO2 Sorbent." Industrial & Engineering Chemistry Research 44:3099-105.

Zhu, YD, HQ Hu, WC Li, and HX Zhao. 2006, "Preparation of Cresol-Formaldehyde Carbon Aerogels Via Drying Aquagel at Ambient Pressure." Journal of Non-Crystalline Solids 352:3358-62.